NOBEL SYMPOSIUM 91 CSNSM report 94-34
Trapped Charged Particles and Related Fundamental Physics
Lysekil, Sweden, August 21-26, 1994
Proc. to appear in Physica Scripta.

The Orsay RF Mass Spectrometer

M. de Saint Simon, C. Thibault, G. Audi, A. Coc, H. Doubre, M. Jacotin, J-F Kepinski, R. Le Gac[1], G. Le Scornet, D. Lunney, F. Touchard[1]

Centre de Spectrométrie Nucléaire et de Spectrométrie de Masse, CNRS-IN2P3, F-91405 Orsay-Campus, France

and G.Lebée

Division PPE, CERN, CH-1211 Genève 23, Switzerland

Abstract

A RF mass spectrometer of the L. G. Smith type has been built with 2 aims : to provide an experimental test of the CPT invariance (proton-antiproton mass comparison) and to measure the atomic masses of nuclei far from stability. The features of the spectrometer in the framework of the first application are presented, followed by a discussion on the adaptation to the second one.

PACS number : 29.30.Aj

1. Introduction

A Radio-Frequency Mass Spectrometer (RFMS) based on the same principle as that proposed and realized by L.G. Smith [1,2] was built at Orsay almost 10 years ago in order to measure atomic masses with high precisions. The main advantage of this type of apparatus over classical mass spectrometers is to provide a higher resolving power, thus allowing for elimination of isobaric and even of some isomeric contaminants. An other important advantage is that the RFMS implies measurement of frequency ratios which are inherently more accurate than voltage ratios, as measured by classical mass spectrometers. The latter are limited to 10^{-7} accuracy at best and often suffer systematic errors. Using this technique, L.G. Smith obtained a resolving power of 10^7, and measured stable atomic masses with a precision better than 10^{-9} [3].
The first goal of the Orsay RFMS was to test CPT conservation by comparing the charge-to-mass ratio of H^- ions and of antiprotons ($\overline{p}$)with a precision of 10^{-9}, based on a mass resolving power of 10^6. However the $\overline{p}$ beam with a required kinetic energy as low as 200 keV was not realized at LEAR (Low Energy Antiproton Ring CERN) and the project had to be given up.
Meanwhile, the recent development of the Penning trap has allowed for high precision measurement of individual particles [4] and long lived isotopes such as ^{3}He-^{3}H [5], the mass difference of which is relevant to the neutrino mass determination. In addition, by combining this technique with a time-of-flight measurement [6], a precision of 10^{-7} is reachable if an RF excitation is applied into the trap during 1 second only, thus allowing for mass measurements of short lived nuclei. For shorter times, the resolving power, and then the precision, decreases as the inverse of the duration of the measurement. Conversely, the RFMS being a transmission spectrometer, its performance is not sensitive to the half-life so that it appears to be complementary to the Penning trap technique. It is specifically designed to allow for precise mass measurements (10^{-7}) in the region far from stability which is particularly relevant for nuclear structure model testing, nuclear binding energy determination in "halo nuclei", and astrophysics calculations based on the r-process path.
This paper presents the main features of the antiproton mass configuration of the RFMS with special emphasis on the radiofrequency part which has not yet been described, and a brief discussion of the modifications required to adapt it for atomic mass measurements.

2. The RFMS

1.1 RFMS principle

The RFMS aims to compare masses of species A and B through the comparison of the cyclotron frequencies ν_{cA} and ν_{cB} of their ions rotating alternately in the same homogeneous magnetic field B_0. Classically, one has :

$$\nu_c = qB_0 / 2\pi m. \qquad (1)$$

If the trajectories of ions A and B are identical, and if the field is stable enough versus time, the ionic masses and the cyclotronic frequencies obey the relationship :

$$m_A \nu_{cA} = m_B \nu_{cB}. \qquad (2)$$

The RFMS consists essentially of a magnet providing a highly homogeneous magnetic field in a cylindrical gap, a four-fold radiofrequency cavity, and two symmetrical beam lines for the injection and the ejection of the ions (Fig.1). The ions enter the magnetic field through the inlet slit, make two turns in the magnetic field following to an helicoidal trajectory and are then deflected through the exit slit. At the end of the 1st and 3rd half-turn, the ions pass the slits and cavities of the RF modulator so that their kinetic energy T_0, and thus the radius of their trajectory :

[1] Present address : Centre de Physique des Particules de Marseille, CNRS-IN2P3, Luminy F-13288 Marseille, France

$$R_0 = \sqrt{2mT_0} \ / \ qB_0, \qquad (3)$$

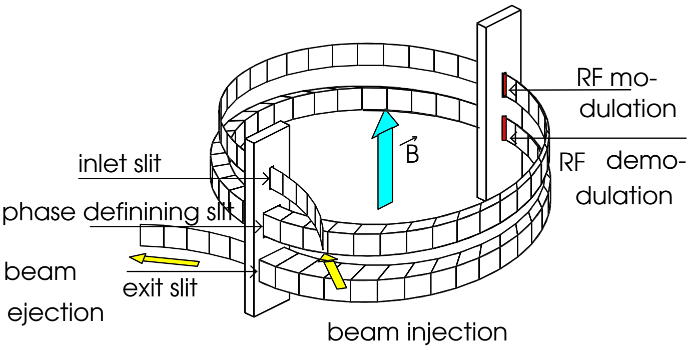

Fig. 1. The RFMS principle. The beam envelope is displayed for a modulation frequency out of resonance.

is modified according to the phase of the RF when they cross the modulator. The resulting effect is to spread the ionic beam which almost do not pass the exit slit (Fig.1). However, since ν_c does not depend on the kinetic energy, it is possible to tune the radiofrequency in order to get opposite phases between the two crossings so that the second modulation exactly cancels the first one for all ions.

In that case, the transmission is again at maximum. The "resonance" condition is given by :

$$\nu = (n + 1/2)\nu_c \qquad (4)$$

where n is an integer. By measuring the transmission versus ν narrow peaks are obtained around each resonance value. A "phase defining slit" is inserted half-way between the two modulations (Fig.1) in order to stop the ions which received the maximum modulation and which are responsible for tails around the resonance peak. The mass resolving power may be calculated [7] as :

$$\mathcal{R} = \frac{m}{\Delta m} = 2\pi n \frac{D_m}{w} \frac{A_\delta}{R_0} \qquad (5)$$

where D_m is the amplitude of modulation of the diameter of the trajectory, w is the slit width, and A_δ is the dispersive power of the injection and ejection lines. It is here implicitly assumed that the isochronism of the trajectories, which depends on the magnetic field homogeneity, is not a limiting factor.

1.2 The RFMS set-up for $H^-/\bar{p}$ mass comparison

The main characteristics are compiled in Table 1 and the whole device, including a H^- ion source running at 200 kV, is shown in Fig. 2. The H^- ion beam is swapped with the antiproton beam by using a pulsed electrostatic deflector. The injection and ejection lines are fully symmetric. All their elements are electrostatic so that their potentials must be switched according to $m_A V_A = m_B V_B$ when the ionic beam is switched from species A to B. The two beams can therefore follow the same trajectory without changing the magnetic field. Each line includes two 90 degrees spherical sectors which constitute an energy filter, a cylindrical deflector used to bend the trajectory in order to spare space, various components (hexapoles, quadrupoles and dipoles) which focus and drive the beam inside the fringing field of the magnet, and

Table I. Main technical data for the design of the RFMS

$\bar{p}$ kinetic energy	T_0	200 keV
Magnetic induction	B_0	0.13 T
Mean orbit radius	R_0	500 mm
Pole internal radius		330 mm
Pole external radius		670 mm
Magnet gap		140 mm
Magnet weight		25 tons
Cyclotron frequency	ν_c	2 MHz
RF frequency	ν	3 GHz
Harmonic number	n	1500
Modulation amplitude	D_m	5 mm
Width of the slits	w	0.2 mm
Height of the slits	h	5 mm
Width of the phase defining slit		5 mm
Energy dispersive power of filters	A_δ	3 000 mm
Foreseen resolving power	$\mathcal{R}$	10^6

a cylindrical injector (or ejector). The energy filters have a high dispersive power A_δ and a linear magnification of 1.

The 25 ton magnet was designed to provide a magnetic field between 0.10 and 0.80 T. Using both magnetic shimming and pole face coils, the required homogeneity for a resolving power of 10^6 was obtained [8]. The detector is a high gain electron multiplier used in counting mode. All RFMS parameters are controlled by a dedicated computer which also insures data acquisition. The design parameters lead to a theoretical

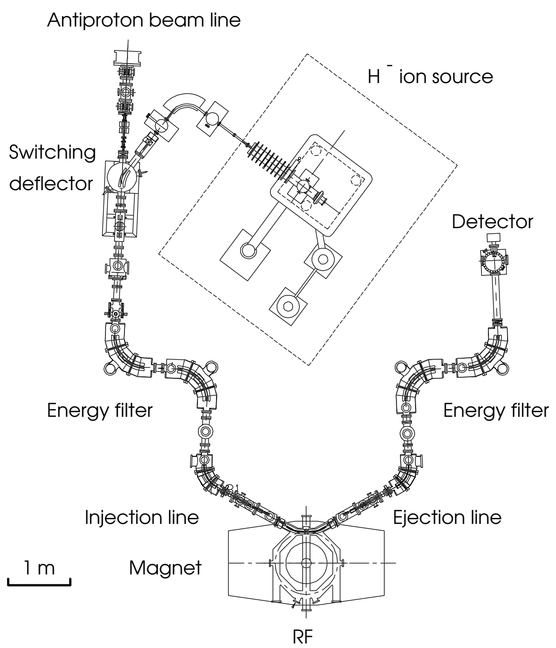

Fig. 2. The RFMS set-up for the $H^-/\bar{p}$ mass comparison at LEAR (CERN).

resolving power of 1.4 x 10^6. A multi-particle simulation shows that the resolving power is limited, because of secondary effects, to around 10^6.

2. The RF System

2.1 The RF modulator

The purpose of the modulator is to produce an electric field inside the volume delimited by the slit aperture and the thickness of the accelerating gap g (Fig. 3). The gap must be

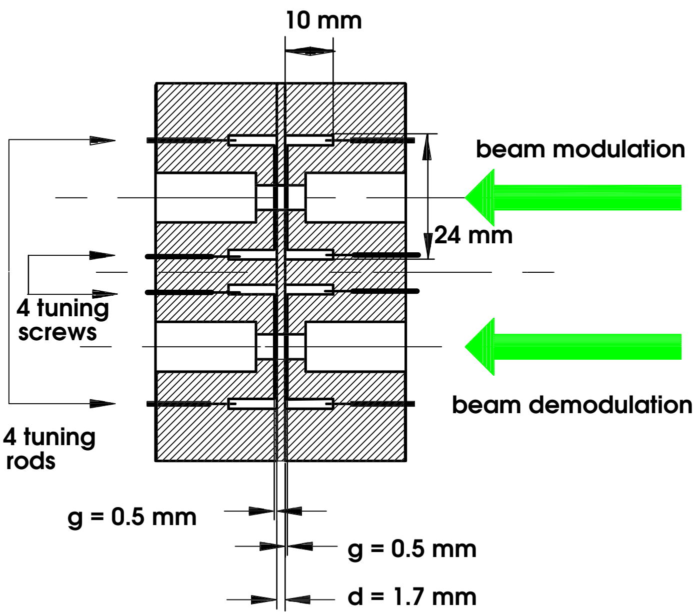

Fig. 3. The RF modulator. Four other tuning rods are not visible.

as small as possible to avoid deterioration of isochronism between the modulation and the demodulation. The amplitude of the electric field E_0 must be sufficient to modulate the diameter of the trajectory D_m by 5 mm (0.5 %). To avoid sparks E_0 should be limited and two cavities separated by a drift section d are to be used for modulation and demodulation. The efficiency of the double modulation system is maximum when

$$d + g = \beta\lambda / 2 \qquad (6)$$

where $\beta = v / c$ (v ion velocity) and λ is the RF wave length. With g = 0.5 mm and d = 1.7 mm, D_m = 5 mm is obtained with $E_0 = 2 \times 10^6$ V/m. This geometry leads to the construction of a four-fold resonant cavity with the requirement to get the same electric field amplitude in the four cavities and a homogeneity of the field in the gaps of 10^{-3}.
Each cavity is equivalent to a portion of coaxial line terminated at one end by a short circuit and at the other end by a circular shaped-capacitor. A slit at the center of the capacitor lets the beam enter the accelerating gap between the plates. The size of the cavities is adjusted to get a resonance frequency of 3027 MHz. The quality factor Q is 1300 and the dissipated power is 60 W (for $E_0 = 2 \times 10^6$ V/m), requiring water cooling of the modulator. The four-fold cavity is fed with the RF field through 4 coupling apertures. They are located symmetrically versus the two guide axes allowing for the coupling of the four cavities with the same phase (mode H01). Four tuning screws are used to allow coarse tuning. To get the same amplitude in the four cavities, two remotely adjustable rods are installed in each of them : one to adjust the resonance and the other to modify the aperture of the RF injection window.
The RF power coming from a klystron is driven through a wave guide and injected inside the apertures through a $\lambda/4$ transformer. Its purpose is to lower the Q factor and to decrease the sensitivity of the resonance frequency to room temperature. The size of the coupling apertures has been reduced (undercoupling) to get rid of perturation of the electric field distribution that is responsible for sparks. The impedance mismatch of the cavities and the $\lambda/4$ transformer produces a reflected wave ($\rho = 0.5$) and the overall Q factor is lowered to 130. A 3 MHz (-3 dB) bandwidth is obtained. As a consequence, more power is required from the amplifier and an insulating device has to be inserted for protection.

2.2 *The RF power injection*

The RF signal is generated with a direct synthesis generator allowing for fast frequency switching which is under the control of the data acquisition sytem. In order to cover the working frequency range, it is followed by a frequency doubler. A one watt preamplifier stage is used to feed a 1 kW klystron working between 3020 and 3030 MHz. The reflected power is absorbed in an insulator device and the power is transmitted to the wave guide through a 5 meter long coaxial cable. The wave guide terminated by the four-fold cavity enters the vacuum chamber through a ceramic window. A watt-meter and a network analyser are to be used to make the fine tuning of the cavities of the klystron. To get the required electric field $E_0 = 2 \times 10^6$ V/m, the klystron must produce a power of 400 W.

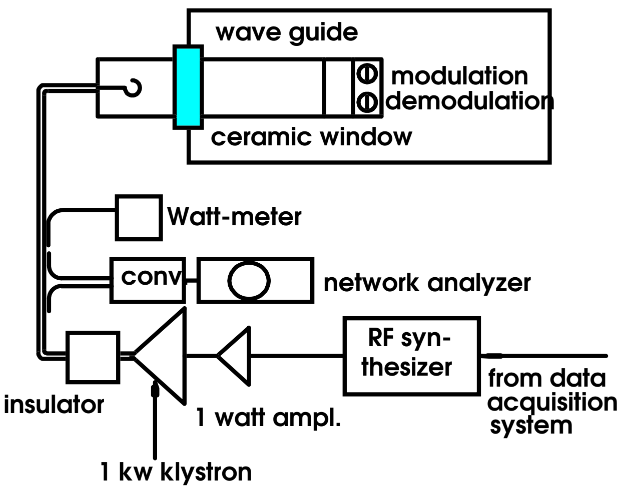

Fig. 4. The RF power system for the RFMS.

3. The RFMS features

All the features of the spectrometer, due to the lack of $\overline{p}$ at the right energy, have been measured with the H^- beam.

3.1 Beam transmission

The beam transmission is an important feature as it governs the statistics available in the mass peak. It is related to the incoming beam emittance ε and to the RFMS acceptance (a_H, a_V, a_E respectively horizontal, vertical and energy acceptance, Table 2). It can be roughly estimated by the formula :

$$T = \left[1 - \exp\left(-\frac{3a_H}{\varepsilon_H}\right)\right] \times \left[1 - \exp\left(-\frac{3a_V}{\varepsilon_V}\right)\right] \times \left[\mathrm{erf}\left(\frac{a_E}{\sigma_E\sqrt{2\pi}}\right)\right] \times \frac{2\Phi_0}{\pi} \times t_s^8$$

(7) where the four first terms correspond to the horizontal, the vertical, the energy and the RF phase losses, σ_E is the variance of the energy distribution and Φ_0 is the phase acceptance of the phase defining slit. Finally, the last term t_s stands for the losses due to beam aberrations in the 8 slits of the system. The experimental value of the transmission is highly sensitive to the setting of the large number of parameters driving the trajectory. The optimal setting-up leads to a transmission of 5 x 10^{-5} in agreement with the estimation from the formula.

Table II. RFMS acceptance and H^- beam emittance.

RFMS acceptance :	H^- beam emittance :
$a_H = 1\ \pi$ mm mrad	$\varepsilon_H = 8\ \pi$ mm mrad
$a_V = 2\ \pi$ mm mrad	$\varepsilon_V = 8\ \pi$ mm mrad
$a_E = 12$ eV	$\sigma_E = 125$ eV
$t_s = 0.75$	
$\Phi_0 = \pi/6$	

3.2 Mass resolving power

The mass peak is recorded making an histogram of the counting rate versus the frequency. To optimize the resolving power R the RF modulator must be accurately tuned so as to achieve a sufficiently large modulation of the diameter of the trajectory. This modulation can be adjusted by the RF power settings which require a fine tuning of the klystron cavities. The amplitude is directly determined by measuring the intensity profile of the beam in the adjustable aperture of the phase defining slit. The next step is to get the same amplitude of the electric field in the four cavities as the inequality is responsible for a broadening of the mass peak.

The determination of the peak width is the most sensitive test of the correct tuning of the modulator. The data analysis system provides an evaluation of the full width at half-maximum of the peak (Fig. 5). It is evaluated through a fit of two symmetric straight lines across the experimental points since the expected shape is triangular [7]. The mass resolving power has been measured to be 8.3 x 10^5, a value reasonably close to the designed one. The main problem is related to the bandwidth of the RF system which forbids moving from one harmonic to the next without changing the modulation amplitude.

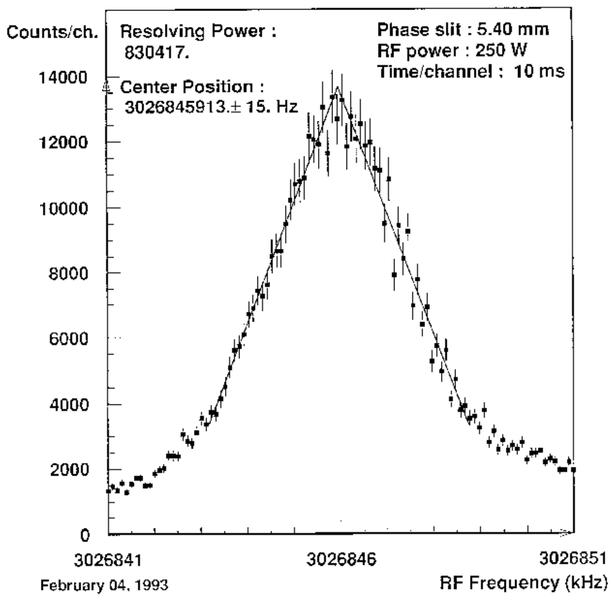

Fig. 5. An example of a H^- mass peak for which a resolving power of 8.3 x 10^5 is measured. The symmetry center of the peak is determined with an accuracy of 5 x 10^{-9}.

3.3 Enhancement factor

For application of the RFMS other than mass measurements, the enhancement factor related to the peak shape far from center is an important feature. For that purpose, the ratio of the ion current at the central frequency and at a frequency shift $\nu_c / 4$ has been measured to be 10^8. It could allow for detection of a very small amount of material with a mass shift of 1.8 x 10^{-4}. This feature is interesting for beam purification. As an application, the preparation of targets made of the pure isomeric state of ^{178m2}Hf is under discussion.

4. Adaptation to atomic mass measuremens

As the $\bar{p}/H^-$ mass comparison is no longer considered, modifications have been undertaken to adapt the RFMS to heavier mass measurements. Taking advantage of the very short transit time (≈ 50 µs), which is a crucial advantage over Penning traps, we plan to measure masses of very short-lived nuclei ($T_{1/2} \leq 1$ s) produced by the ISOLDE facility at CERN. The mass range extends from A = 7 up to 250. In order to get a precision of 10^{-7}, the resolving power may be reduced, down to 10^4. However, the ISOLDE beam may contain isobar contaminants which must be separated, so that a resolving power of 10^5 is desirable. This value is reachable with $A_\delta = 1$, so that the energy filters may be removed. This improves the acceptance, and then the transmission, which is an essential parameter since the most interesting nuclei are those further from stability, where the yields from on-line separators are progressively weaker. For this reason, the size of the four remaining slits, including the modulator ones, will be enlarged to 0.4 x 10 mm^2. The transmission for the ISOLDE beam is then evaluated as ≈ 1 %. The removal of the filters also makes the set-up relatively more compact (Fig. 6).

4.1 The ion source

The ISOLDE ionic beam has a nominal kinetic energy of 60 keV so that a new auxiliary ion source running at 60 keV has to be installed to provide a permanent test beam during the RFMS setting-up (plasma ion source), and to supply the mass reference beam (electron impact ion source) during the actual mass measurements.

4.2 The magnet

The RFMS magnetic field will be increased to 0.8 T and will allow for measurements at 60 keV for masses up to A = 100, while for heavier masses up to 250, the kinetic energy will have to be progressively reduced from 60 keV to 30 keV. The field mapping at 0.8 T performed without the pole face coils, has shown a field homogeneity compatible with a resolving power of 10^5 [10].

4.3 The RF modulator

Since the masses are heavier, ω is reduced and the frequency range may be lowered to 250 - 500 MHz, resulting in a new design of the RF modulator. In order to match the mass range from A = 7 up to 250, four models of the modulator are needed with different gap and drift lengths.

5. Conclusions

A radio-frequency mass spectrometer has been constructed according to the principle of L. G. Smith. The mass resolving power and the transmission have been measured to be close to the designed values. Since the 200 keV $\overline{p}$ beam required to make the mass comparison of $\overline{p}/H^-$ could not be realized, the spectrometer is currently under transformation to fit the requirements of atomic mass measurements of nuclei far from stability.

Aknowledgements

We are grateful to F. Bergsma, W. Flegel, P. A. Giudici, P. Knobel, G. Petrucci, R. Rey-Mermier and G. Stefanini (PPE division CERN) for their contribution to the magnetic measurements and to E. Haebel (AT division, CERN) for fruitful discussions about the RF design of the modulator.

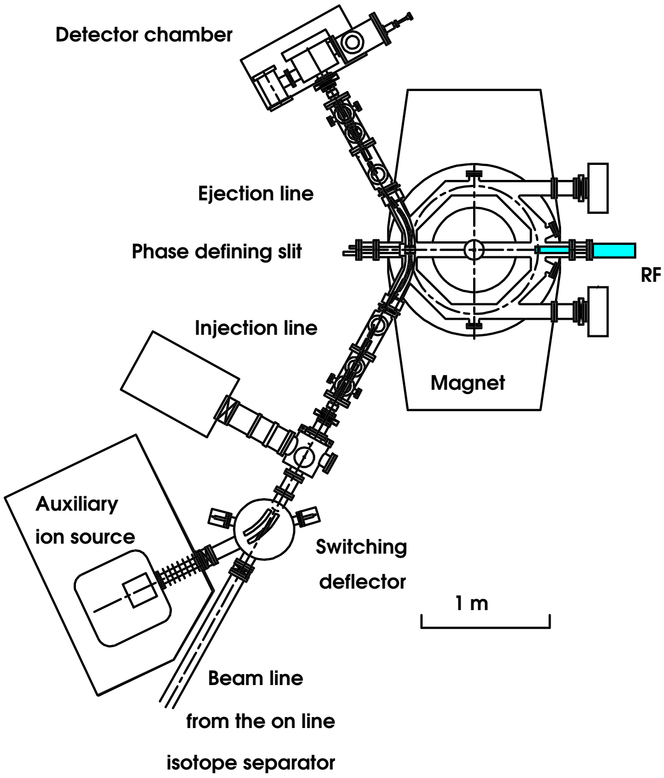

Fig. 6. Layout of the RFMS in the atomic mass measurement configuration.

References

[1] Smith, L. G., Proc. Int. Conf. on Nuclidic Masses, ed. H. E. Duckworth (Univ. of Toronto Press, Canada, 1960) p.418.
[2] Smith, L. G., Proc. 3rd Int Conf. on Atomic Masses, ed. R. C. Barber (Univ. of Manitoba Press, Winnipeg, Canada, 1967) p. 811.
[3] Smith, L. G., Phys. Rev. C**4**, 22 (1971).
[4] Jhe, W., Phillips, D., Gabrielse, G., Grobner, J. and Kalinowsky, H., Physica Scripta **46**, 268 (1992).
[5] Van Dyck, R. S. Jr., Farnham, D. L. and Schwinberg, P. B., Proc. 6th Int. Conf. on Nuclei Far From Stability and 9th Int. Conf. on Atomic Masses and Fundamental Constants. Inst. Phys. Conf. Ser. No 132, p.3.
[6] Otto, T. et al., Nucl. Phys. A**567**, 281 (1994).
[7] Coc, A., Le Gac, R., de Saint Simon, M., Thibault, C. and Touchard, F., Nucl. Instr. Meth. A**271**, 512 (1988)
[8] Coc, A. et al., Nucl. Instr. and Meth. A**305**, 143 (1991).
[9] Touchard, F., Huber, G., Fergeau R., Thibault, C. and Klapisch, R., Nucl. Instr. and Meth. **155**, 449 (1978).
[10] Bergsma, F. et al., Internal report CSNSM 94-24 , F-91405 Orsay-Campus.